Nanomechanical Characterization of *Bacillus anthracis* Spores Using Atomic Force Microscopy

Alex G. Li [a], Larry W. Burggraf [a], and Yun Xing [b]

Department of Engineering Physics, Air Force Institute of Technology, 2950 Hobson Way, WPAFB, OH, 45433, USA[a]

Oak Ridge Institute for Science and Education (ORISE), 1299 Bethel Valley Road, Oak Ridge, TN 37830[b]

Supplementary Materials: Additional figures

Figure s1 shows an indented spore with three nearly symmetric side surfaces, labeled by X, Y, and Z (see Fig.s1d). The surface region (X) is obviously correlated to the front surface of the corner cube indenter; the surface regions (Y and Z) are correlated to two side surfaces of the indenter (Fig.1a).

14

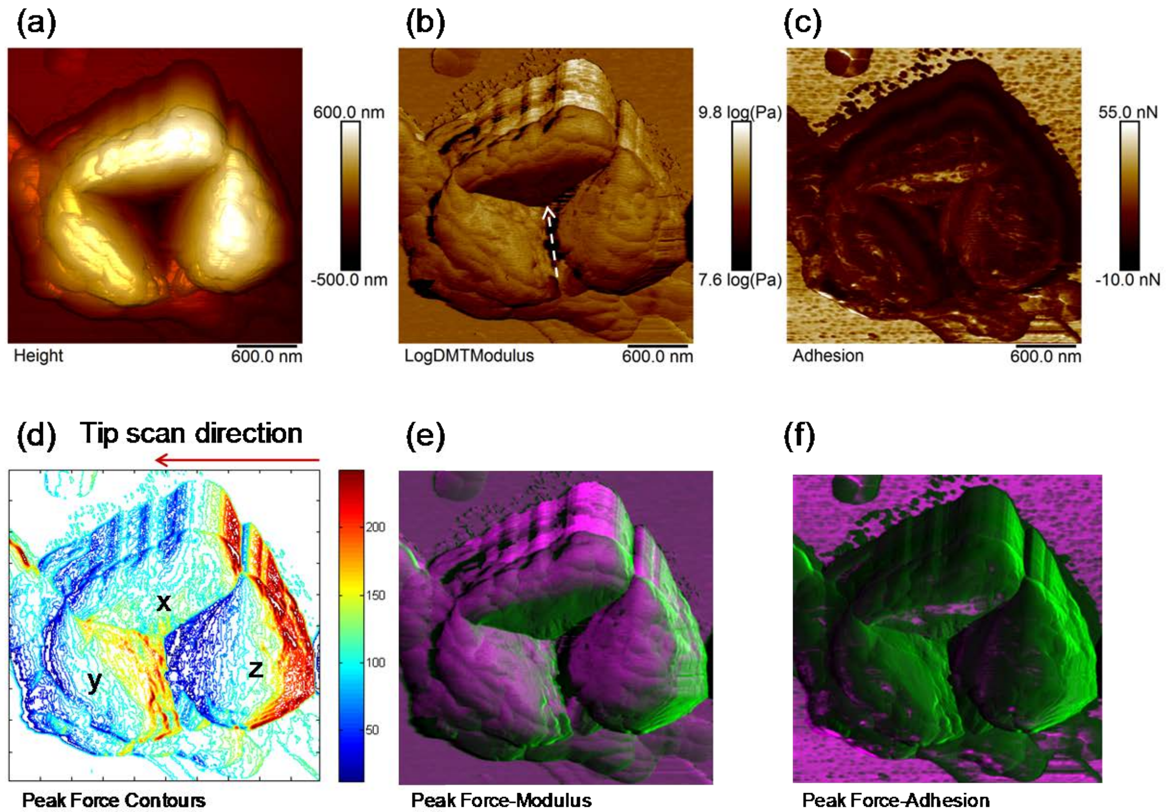

15 Figure s1 AFM images of a fractured spore section (#2) on the mica surface at room temperature
16 in air. (a) Height, (b) Modulus on the logarithmic scale, (c) Adhesion, (d) Peak force contour, (e)
17 Overlay of peak force and modulus, and (f) Overlay of peak force and adhesion. The AFM
18 images are plane-fitted using the line by line algorithm, and rescaled for visual clarity. AFM
19 parameters are as follow. Scan size: 3.0 um, scan rate: 1Hz, samples/line: 512, line direction:
20 retrace, capture direction: down, scan angle: 90 degrees, control gain: 21, amplitude setpoint: 20
21 nN, and drive amplitude: 120 nm at 2 kHz. Spring constant: 2.5 N/m. Tip radius: 30 nm. The
22 modulus corrected using the linear ratio analysis for the different regions, X, Y and Z, are 1, 3.9,
23 and 4.2 GPa, respectively.

24

25 To illustrate the line-cut method, we show the AFM height and peak force images of a
26 cluster of spores before and after they were cut using the diamond tip. There were about six

spores of different sizes and two segments of the residual cells that can be identified in Fig.s2. The spores showed an oval or spherical shape depending upon their orientations on the surface. The residual cells left in the sporulation process showed a long, collapsed tubular shape. One was oriented in the horizontal (top) and the other in the vertical direction (left), which were distinctly different from the spores. The diamond tip cut through 3 spores in the vertical direction, producing fractured surfaces along the cutting line, as highlighted by the arrows in Fig.s2f.

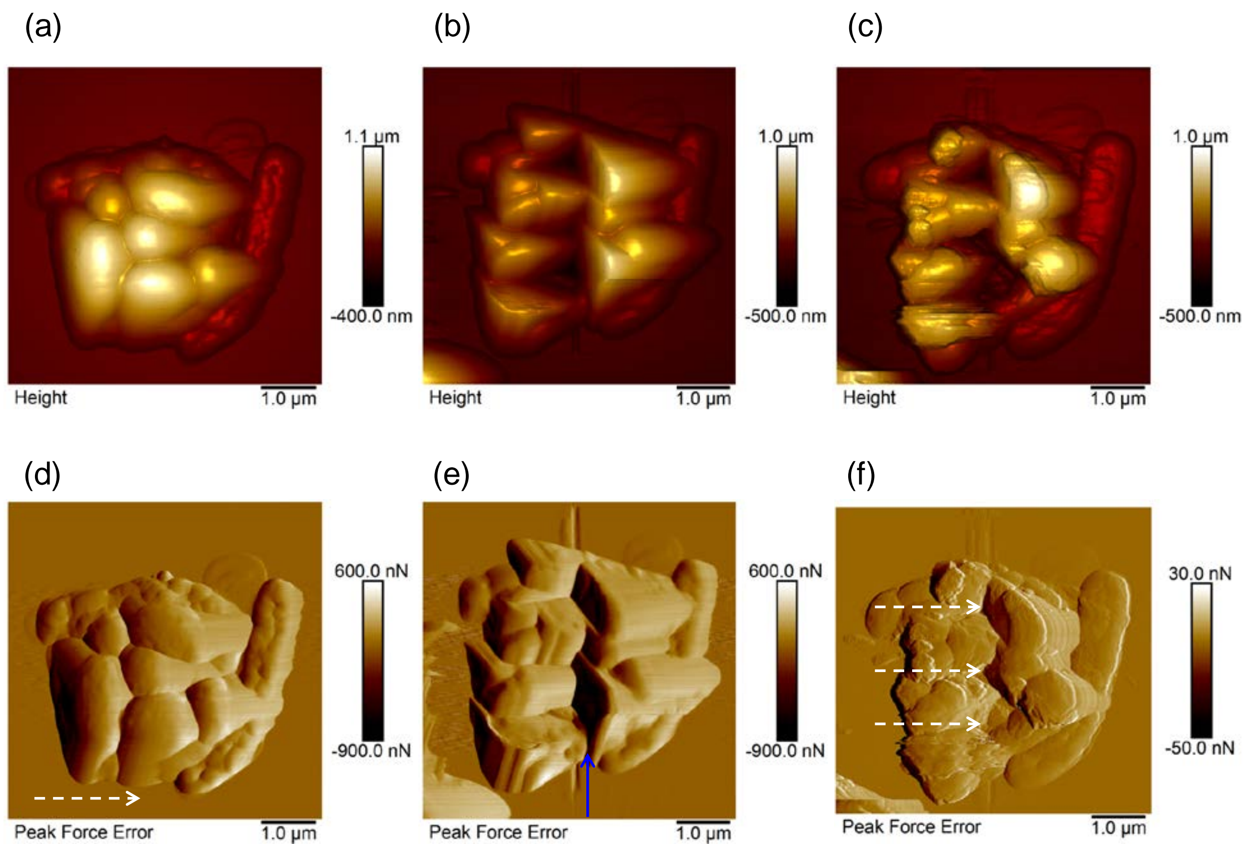

Figure s2 AFM images of selected spore samples produced by the line-cut method on mica substrates. The top row shows the height images of the spores before (a) and after (b and c) they are cut by the diamond AFM tip along a vertical line in the y-axis direction (blue arrow in e). The bottom row shows the corresponding peak force images of the spores before (d) and after (e

39 and f) they are cut by the diamond AFM tip. The diamond cantilever tip is aligned in the arrow
40 direction (d). The fractured sections of three spores are highlighted by the arrows (f).
41
42 The top row images in Fig.s3 are the topographic surface (a), modulus (b), adhesion (c),
43 and deformation (d) of a spore (white arrow) and a piece of the residual cell wall (blue arrow).
44 The freshly cut spore appeared to be attached at the end of the cell wall. The top row images (a-
45 d) are the height, modulus, adhesion, and deformation, respectively. The spore, located at the
46 lower portion of the image, was indented with the diamond tip, as highlighted by the white arrow
47 in s3a. The bottom row images (e-h) are the height, modulus, adhesion, and deformation image
48 of the spore section recorded at a higher resolution. The images were plane-fitted using the line
49 by line algorithm and rescaled for visual clarity. The lighting effects are used to enhance the
50 visual depth of the height images: incident light in the positive y-axis direction and at 25 degrees
51 off the x-y plane.
52
53

54

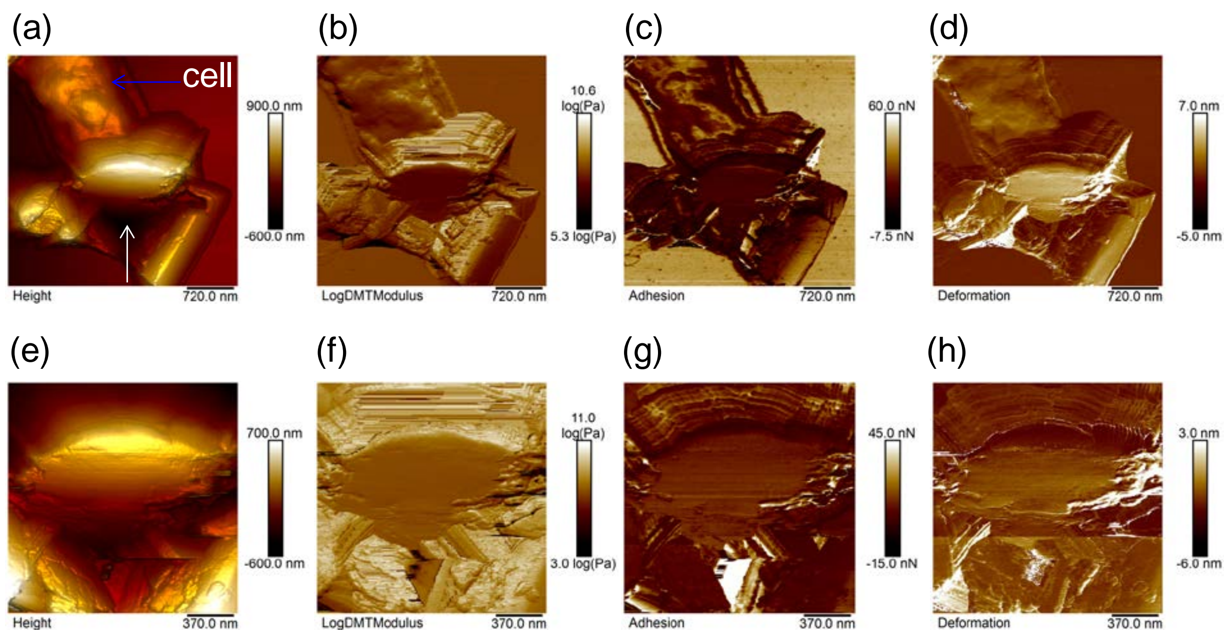

55 Figure s3 AFM images of a freshly cut spore attached to the bacterial cell on the mica surface.
56 The top row includes the low resolution height (a), modulus (b), adhesion (c), and deformation
57 (d) image. The bottom row shows the higher resolution images of the spore section: height (e),
58 modulus (f), adhesion (g), and deformation (h) image of. The images are plane-fitted using the
59 line by line algorithm and rescaled for visual clarity. The lighting effects are used to enhance the
60 visual depth of the height images: incident light in the positive y-axis direction and at 25 degrees
61 off the x-y plane. The cutting diamond tip was aligned in the positive y-axis direction. The
62 freshly exposed section of the spore is highlighted by the white arrow in Fig.s3a. The AFM
63 parameters for Fig.s3a-d are as follow. Scan size: 3.6 um, scan rate: 1Hz, samples/line: 512, line
64 direction: retrace, capture direction: down, scan angle: 90 degrees, control gain: 15, amplitude
65 setpoint: 25 nN, and drive amplitude: 120 nm at 2 kHz. Spring constant: 2.5 N/m. Tip radius: 30
66 nm. The AFM parameters for Fig.s3e-h are as follow. Scan size: 1.8 um, control gain: 10,
67 amplitude setpoint: 3 nN. Other parameters are the same to Fig.s3a-d.

68

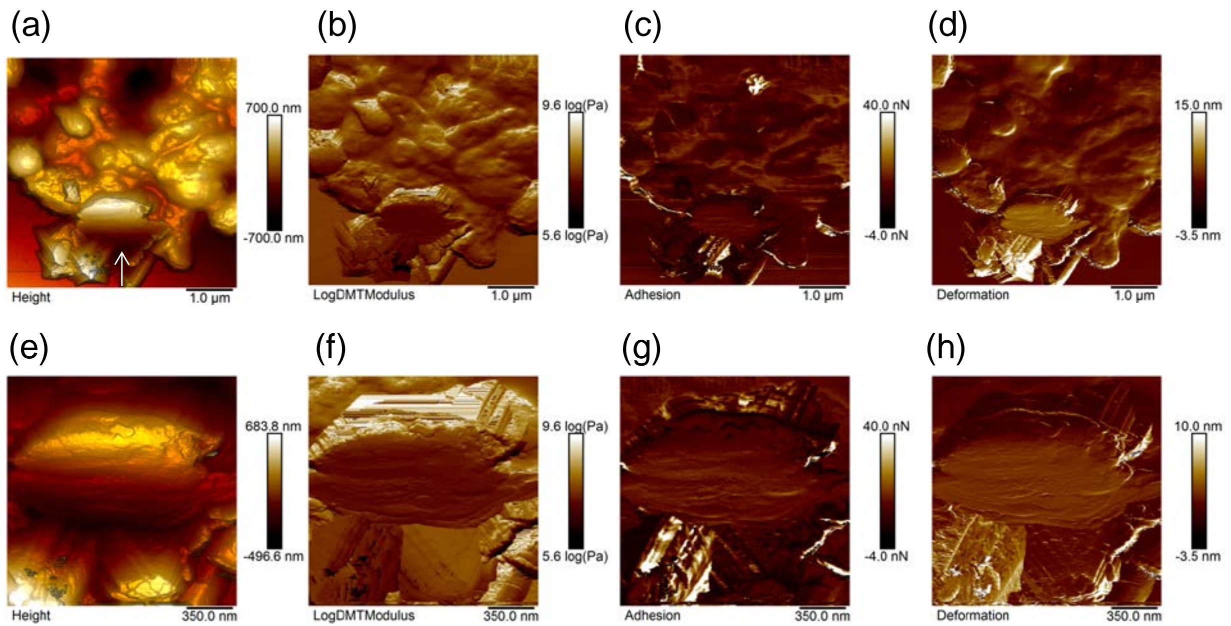

Figure s4 AFM images of a freshly cut spore attached to the edge of a large cluster of the spores and probably the bacterial cell walls on the mica surface. The top row images (a-d) are the height, modulus, adhesion, and deformation, respectively. The spore, located at the lower portion of the image, was indented with the diamond tip, as highlighted by the white arrow in Fig.s4a. The bottom row images (e-h) are the height, modulus, adhesion, and deformation image of the spore section recorded at a higher resolution. The images are plane-fitted using the line by line algorithm and rescaled for visual clarity. The lighting effects are used to enhance the visual depth of the height images: incident light in the positive y-axis direction and at 25 degrees off the x-y

84 plane. The AFM parameters for Fig.s4a-d are as follow. Scan size: 5.0 um, scan rate: 1Hz,
85 samples/line: 512, line direction: retrace, capture direction: down, scan angle: 90 degrees, control
86 gain: 16, amplitude setpoint: 30 nN, and drive amplitude: 120 nm at 2 kHz. Spring constant: 2.5
87 N/m. Tip radius: 30 nm. The AFM parameters for 7e-h are as follow. Scan size: 1.5 um, control
88 gain: 9, amplitude setpoint: 3 nN. Other parameters are the same to Fig.s4a-d.

89

90

91

92

93

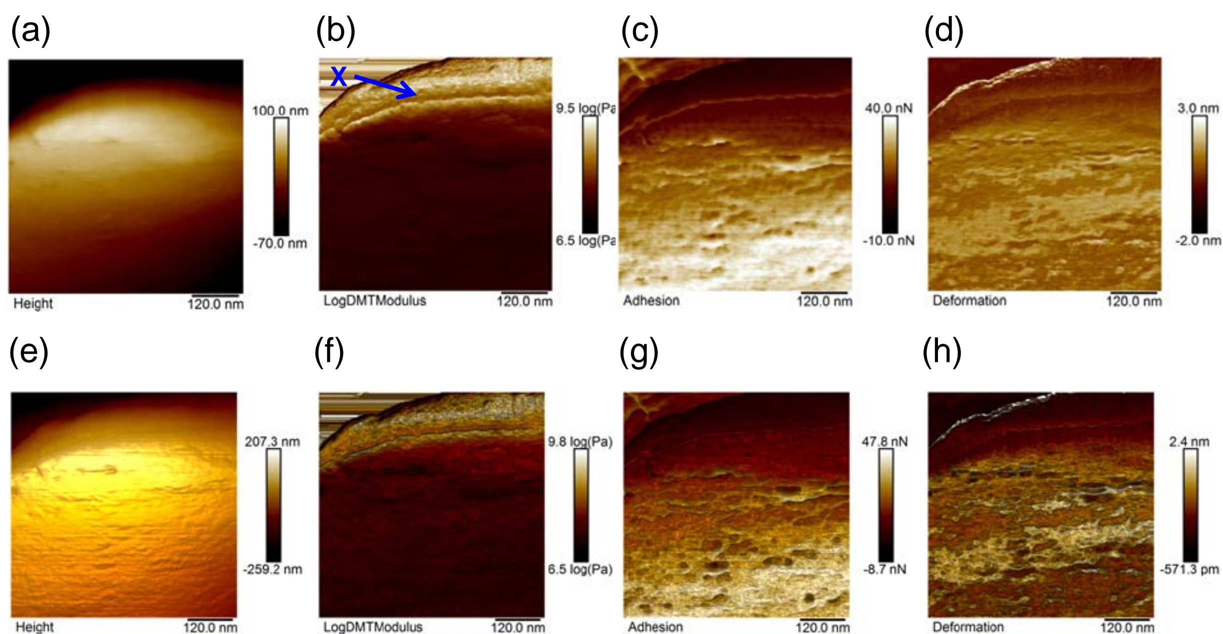

94

95

96 Figure s5 High resolution AFM images of the cross-section of the spore displayed in Fig.s3. The
97 upper row images without the light illumination: (a) Height, (b) Modulus on the logarithmic
98 scale, (c) Adhesion, (d) Deformation. The lower row images are the same to Fig.s5a-d except for

99 the light illumination. The boundary-like feature is indicated by the arrow (Fig.s5b). All of the
100 images have been plane-fitted and rescaled for clearer view. The spore was imaged at the same
101 angle used in Fig.s4. Scan size: 615 nm, scan rate: 1Hz, samples/line: 512, line direction: retrace,
102 capture direction: down, scan angle: 90 degrees, control gain: 8, amplitude setpoint: 1.2 nN, and
103 drive amplitude: 120 nm at 2 kHz. Spring constant: 0.5 N/m. Tip radius: 10 nm.

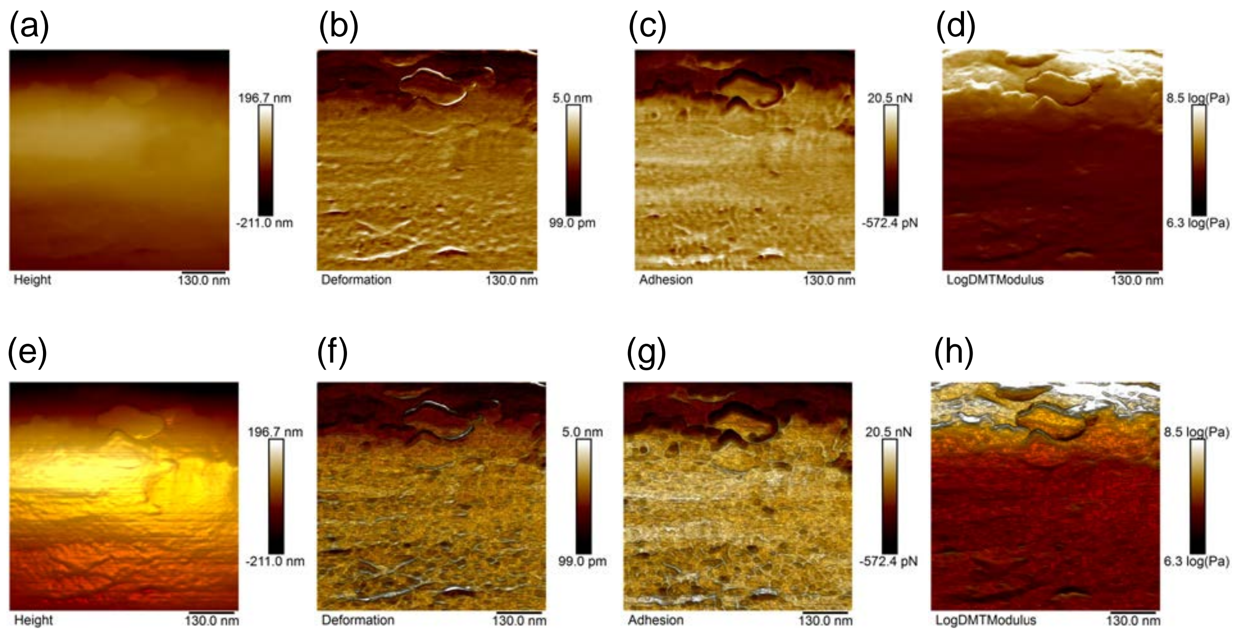

104

105

106 Figure s6 High resolution AFM images of the cross-section of the spore displayed in Fig.s4. The
107 top row includes the height (a), modulus (b), adhesion (c), and deformation (d). The bottom row
108 shows the same images with the illumination effect. The images are plane-fitted using the line by
109 line algorithm and rescaled for visual clarity. The lighting effects are used to enhance the visual
110 depth of the height images: incident light in the positive y-axis direction and at 25 degrees off the
111 x-y plane. The AFM parameters are as follow. Scan size: 664 nm, scan rate: 1Hz, samples/line:
112 512, line direction: retrace, capture direction: up, scan angle: 90 degrees, control gain: 10,

113 amplitude setpoint: 1.5 nN, and drive amplitude: 120 nm at 2 kHz. Spring constant: 0.5 N/m. Tip
114 radius: 10 nm.

115 It should be pointed out that the surface morphology and nanomechanical properties of an
116 inclined surface spore section can significantly differ from those of a horizontal spore section. A
117 great caution must be taken when interpreting the AFM topographic and property images
118 obtained on the inclined surface. For example, the surface features of the slope plane may appear
119 to be compressed, smaller than the actual size, in the direction normal to the inclination because
120 the image is recorded at a projected angle. More importantly, the force applied by the AFM
121 piezoelectric transducer on a tip that climbs up a sharp slope is larger than the force applied on a
122 tip that descends the slope, as shown in Fig.s7. The convolutions between the applied force,
123 surface slope, and scan direction can introduce significant artifacts in the modulus image of
124 inclined surfaces. To give a more specific example, we plot in Fig.s7d the height (red), peak
125 force (green), and the first derivative of the height (black, averaged over 5 data points), which
126 are obtained on a polystyrene surface having a series of parallel ridges and troughs using a
127 silicon tip (Fig.s7a). As the tip scans the polymer structures from the right to left (e.g. retrace) at
128 a fixed y-axis position, as indicated by the dotted arrow (Fig.s7c), the peak force increased
129 sharply above its baseline value upon climbing the steep ridge; it dropped quickly below its
130 baseline value upon descending from the ridge. We found that the peak force was nearly in
131 perfect correlation with the first derivative (or slope) of the height in the direction of the
132 scanning tip. The changes in the modulus for the retrace and trace curve are shown in Fig.s7e.
133 There was a sharp positive spike in the modulus as the tip climbs up the nano-ridge; a sharp
134 negative spike occurred in the modulus as the tip descended the ridge. It is obvious that an
135 increase in the peak force can lead to an overestimated the modulus, while a decrease in the peak

136 force can lead to an underestimated modulus. Since the polystyrene polymer is isotropic, the
137 modulus on both sides of the ridge slopes should be similar. The modulus differences observed
138 in (Fig.s7e) can be attributed mainly to the geometric effect. In addition, the force applied by the
139 tip on the normal direction of the slope is a fraction of the nominal load, depending upon the
140 angle of surface plane. Without the tip slippery, the deformation of the slope may decrease,
141 leading to an overestimate of the modulus. In contrast, if the tip slips on the slope, the
142 deformation of the slope may increase, resulting in an underestimate of the modulus. Therefore,
143 the slope effect must be considered when the modulus changes across the different regions of the
144 spore structures (e.g., core, cortex, and coat) are examined. Despite the presence of the slope
145 effect, the AFM measurements are still invaluable because the nanomechanical information is
146 not assessable by other alternative methods. We believe that the slope effect can be minimized or
147 removed by proper corrections and analysis using experiment and computer modeling. The peak
148 force fluctuations can be reduced by scanning the sample in an appropriate direction. As a first
149 step towards this direction, we explored an equal-contour analysis that may allow us to study
150 changes in the nanomechanical properties at different locations of the spore section.

151 Using the equal contour analysis we described above, it is not difficult to see that the
152 surface (X, Fig.s1d) has a relatively low modulus in comparison with the surrounding spore
153 materials (e.g., Y and Z region). In other words, the three surfaces were not equivalent to each
154 other because the relative strength of the peak force in the X region, as suggested by the green
155 color, was not positively correlated with the peak force contour map, which showed that the peak
156 forces in these regions were comparable. We hypothesize that the observed differences may be
157 due to different modes of deformations in the indented surface regions. It was shown by Atkins
158 and Tabor (1) that the deformation mode of the indented surface changes from the radial cavity

159 expansion to the cutting as the semi-angle of the cone or pyramid indenter is reduced below
160 about 50 degrees. Since the diamond corner cube tip we used to cut the spore can be viewed to
161 have two different semi-angles, a small front (35°) and a large back semi-angle (55°), the spore
162 surface (X) associated with the front side of the diamond indenter may experience a cutting
163 deformation mode, while the spore surface regions (Y and Z) associated with the back side walls
164 of the indenter may undergo a cavity expansion mode. Therefore, only the cutting mode can
165 pierce the coat, exposing the spore section. In contrast, the cavity expansion mode is likely to
166 produce a large indentation in the coat without fracture as the pressure underneath the back
167 surfaces of the indenter is released as the front coat shell is cut open.
168
169
170

171

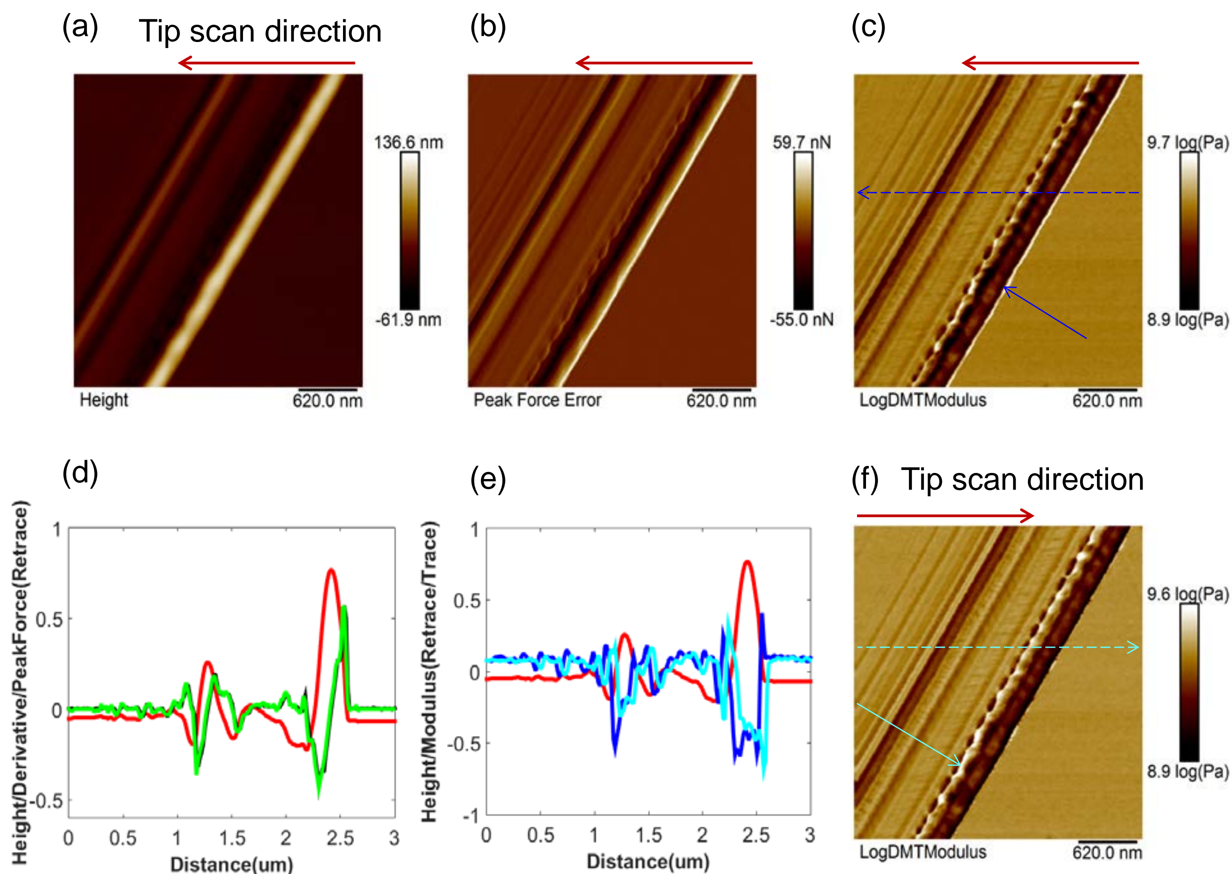

172 Figure s7 AFM height (a), peak force (b), and modulus image (c and f) of the 2MDa polystyrene
173 nanostructures together with changes of the topographic and nanomechanical properties in
174 different directions of the scanning tip. The representative profiles of the height, peak force, and
175 first derivative of the height are shown in red, green, and black in s7d. The direction and location
176 of the scanning tip are indicated by the red and dotted blue arrow in s7c. The profiles of the
177 modulus for the retrace (right to left) and trace (left to right) are indicated by the blue and cyan in
178 s7d. The slope effects on the retrace and trace modulus can also be seen at the nano ridge, as
179 highlighted by the solid blue and cyan arrows in s7c and f, respectively. AFM parameters are as
180 follow. Scan size: 3.1um, scan rate: 1Hz, samples/line=512, line direction: retrace (a, b, c) and

181 trace (f), capture direction: down, scan angle: 0 degrees, control gain: 12, amplitude setpoint: 3.5
182 nN, and drive amplitude: 120 nm at 2 kHz.

183

184 In order to study how the internal structures of spores (e.g., core and cortex) respond to
185 heating at high temperatures for a short duration, we imaged the surface of the spore sample (#1)
186 using a heated AFM tip from the room temperature up to 335 ^{o}C in air. The average heating
187 duration at each point of the surface contact is about 0.5 ms. Figure 13 shows the AFM images
188 of the spore at the room temperature (20°C) before it was heated at 335°C. Again, it is seen in
189 Fig.s8 that the section modulus was lower than the coat (Fig.s8c and g); the section adhesion was
190 higher than the coat (Fig.s8d and h). The AFM images of the spore after it was heated at 335°C
191 are shown in Fig.s9. The striking difference before and after heating at 335°C was the significant
192 increase of the section adhesion force, as indicated in Fig.s9d and h.

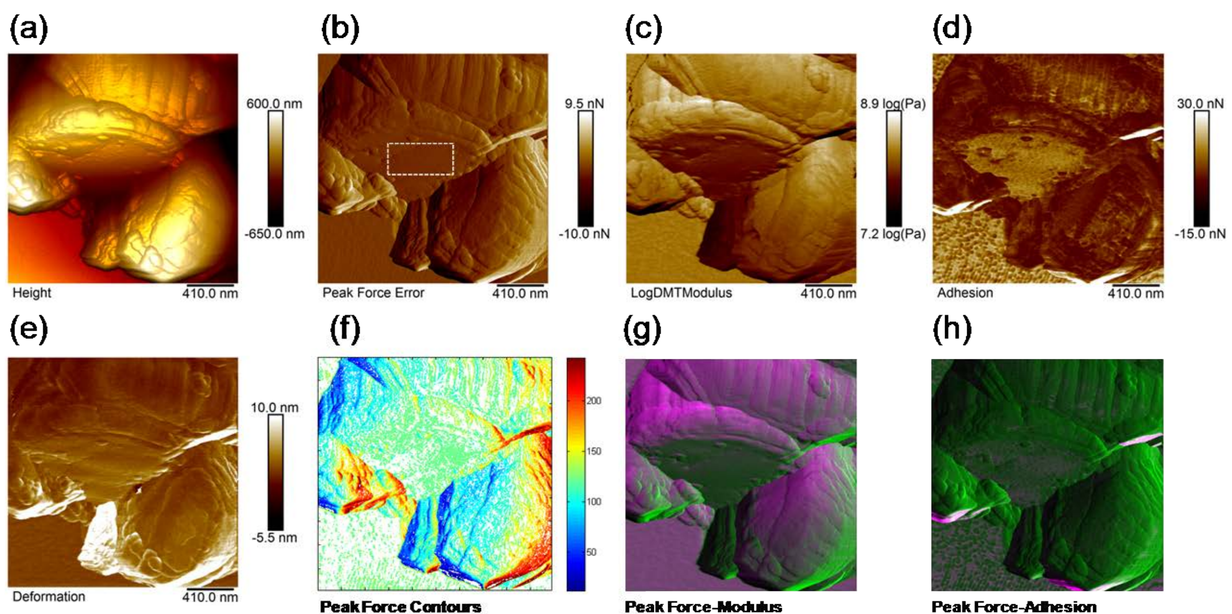

193

194

195

196

197 Figure s8 AFM images of a fractured spore (#5) at 20°C. (a) Height, (b) Peak force, (c) Modulus
198 on the logarithmic scale, (d) Adhesion, (e) Deformation, (f) Peak force contour, (g) Overlay of
199 peak force and modulus, and (h) Overlay of peak force and adhesion. The AFM images are
200 plane-fitted using the line by line algorithm, and rescaled for visual clarity. AFM parameters are
201 as follow. Scan size: 2.1 um, scan rate: 1Hz, samples/line: 512, line direction: retrace, capture
202 direction: down, scan angle: 90 degrees, control gain: 18, amplitude setpoint: 11.5 nN, and drive
203 amplitude: 120 nm at 2 kHz. Spring constant: 2.5 N/m. Tip radius: 30 nm.

204

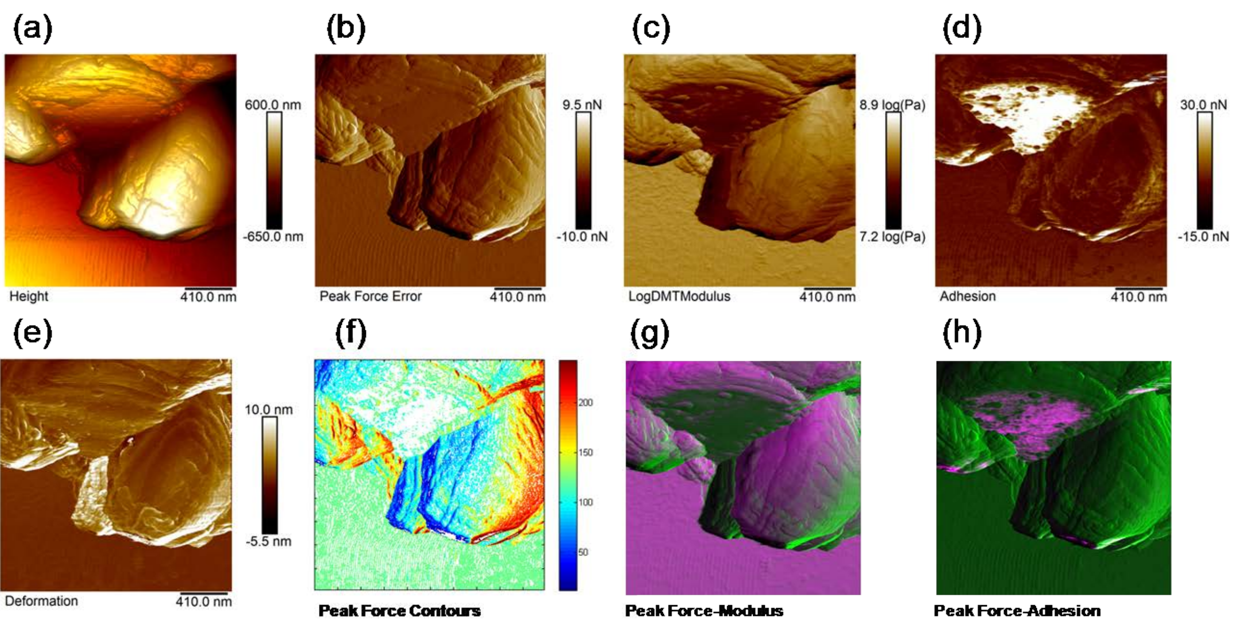

205

206 Figure s9 AFM images of the spore (#5) at 20°C after being gradually heated at 335°C. (a)
207 Height, (b) Peak force, (c) Modulus on the logarithmic scale, (d) Adhesion, (e) Deformation, (f)
208 Peak force contour, (g) Overlay of peak force and modulus, and (h) Overlay of peak force and
209 adhesion. The AFM images are plane-fitted using the line by line algorithm, and rescaled for
210 visual clarity. AFM parameters are as follow. Scan size: 2.1 um, scan rate: 1Hz, samples/line:

512, line direction: retrace, capture direction: down, scan angle: 90 degrees, control gain: 18, amplitude setpoint: 11.5 nN, and drive amplitude: 120 nm at 2 kHz. Spring constant: 2.5 N/m. Tip radius: 30 nm.

1. Atkins AG and Tabor D. 1965. Plastic Indentation in Metals with cones. J. Mech. Phys. Solids 13:149-164.